Transactions of the Materials Research Society of Japan 29[4] 1679-1682(2004)

Magnetic Properties of Sm-Fe-Co-Cu-Nb-B Melt-Spun Ribbons

Mitsuaki Mochizuki, Michihisa Shimizu and Shigeho Tanigawa
Advanced Electronics Research Laboratory, Hitachi Metals, Ltd.
5200 Mikajiri, Kumagayi, saitama, Japan
Fax: 81-48-531-1641, e-mail: mitsuaki_mochizuki@po.hitachi-metals.co.jp

The magnetic properties and crystal structures of Sm-Fe-Co-Cu-Nb-B alloys prepared by melt-spinning technique with a subsequent annealing have been investigated. It is found that Cu addition has different effects on coercivities for different B content alloys. For the alloys of about 8at% B, Cu addition has no effective role and decreases the coercivity of the annealed ribbons. On the other hand, in the range of B=12.5~20.0at%, Cu addition has an essential role not only for increasing coercivities but also for changing the crystal structures. Though the Cu-free ribbons show $Sm_3(Fe,Co)_{62}B_{14}$, $Sm_2(Fe,Co)_{23}B_3$, $Sm_1(Fe,Co)_{12}B_6$ and $Sm_2(Fe,Co)_{14}B_1$ phases, $TbCu_7$ type and $Ce_1Co_4B_1$ type structures appear in the Cu-added ribbons after annealing. The typical magnetic properties of Sm=5.5 at%, B=18.5 at% sample are Br=1.08T, H_{CJ}=0.33MA/m and $(BH)_{max}$=124kJ/m^3. The melt-spun amorphous ribbons were obtained at the roll surface velocity of 4m/s.

Key words: Sm-Fe-Co-Cu-Nb-B, B, Cu-addition, melt-spinning, coercivity

1. INTRODUCTION

From the discovery by Yoshizawa et al.[1] that the Cu addition combined with Nb drastically improves soft magnetic properties, reducing the grain size of the nanocrystalline structure in Fe-Si-Cu-Nb-B (FINEMET) amorphous alloys, several attempts of Cu and Nb additions have been made to improve hard magnetic properties of nanocrystalline exchange spring magnets α-Fe/$Nd_2Fe_{14}B_1$ and Fe_3B/$Nd_2Fe_{14}B_1$. In α-Fe/$Nd_2Fe_{14}B_1$ nanocomposite magnets, Nb addition is widely used for obtaining fine microstructure and to improve magnetic properties[2]. On the other hand, the effect of Cu addition had not been clear. Recent studies of Nd-Fe-Co-Cu-Nb-B alloys show that the Cu, Cu-Nb additions have no effective role to improve the microstructures and magnetic properties in α-Fe/$Nd_2Fe_{14}B_1$ spring magnets[3]. In Fe_3B/$Nd_2Fe_{14}B_1$ spring magnets, it is found that the Cu-Nb addition improves the magnetic properties[4,5]. Detailed study using 3D atom probe analysis and TEM observations[6] on Cu, Nb and Cu-Nb doped α-Fe/$Nd_2Fe_{14}B_1$ and Fe_3B/$Nd_2Fe_{14}B_1$ has clarified that Cu addition to Fe_3B/ $Nd_2Fe_{14}B_1$ is effective in refining microstructure and combined Cu-Nb addition has beneficial effect on the grain size and the hard magnetic properties, though the single Nb addition to Fe_3B/ $Nd_2Fe_{14}B_1$ coarsens the grain size and the Cu addition to α-Fe/ $Nd_2Fe_{14}B_1$ has no beneficial effect in refining microstructure.

Apart from Nd-Fe-B alloys, we previously reported some results concerning the magnetic properties and crystal structures of Sm-Fe-Co-Nb-B melt-spun alloys[7]. The melt-spun ribbons annealed at an appropriate condition are composed of $TbCu_7$ type structure and show hard magnetic properties. Typical magnetic properties of the ribbons annealed at 913 K for 1.5~2.5 h are H_{CJ}=0.55~0.60MA/m, Br=0.85~0.95T, $(BH)_{max}$=120 kJ/m^3 for the composition of $Sm_{6.2}Fe_{bal.}Co_xNb_{2.7}B_{8.3}$ (x=12~16). Though, in ingot state, these alloys are composed of $Sm_2(Fe,Co)_{14}B_1$ and α-(Fe,Co) stable phases, the annealed ribbons show hard magnetic properties and the phase crystallized from amorphous state is $TbCu_7$ type metastable one with the grain size of about 20 nm . In overannealing conditions or outside the suitable range of the compositions, non hard magnetic phasese: $Sm_3(Fe,Co)_{62}B_{14}$, $Sm_2(Fe,Co)_{23}B_3$ cubic phases and planar anisotropic $Sm_2(Fe,Co)_{14}B_1$ or α-(Fe,Co) phases appeared in the ribbons.

In this report, some results concerning Cu addition to $Sm_{6.5}Fe_{bal.}Co_{20}Nb_3B_8$ melt-spun ribbons and more B-rich $Sm_xFe_{bal.}Co_{20}Nb_yB_z$ (x=5.5, 7.0 , y=0, 3.0 z=12.5~20.0) ribbons are presented. These alloy compositions are similar to those of α-Fe/ $Nd_2Fe_{14}B_1$, Fe_3B/ $Nd_2Fe_{14}B_1$ spring magnets if Nd is replaced with Sm and Co is substituted for Fe in the compositions.

For some abbreviations, we use notations 3/62/14, 2/23/3, 1/12/6, 23/6, 3/1, 2/14/1, 1/9, 1/4/1 for $Sm_3(Fe,Co)_{62}B_{14}$, $Sm_2(Fe,Co)_{23}B_3$, $Sm_1(Fe,Co)_{12}B_6$, $(Fe,Co)_{23}B_6$, $(Fe,Co)_3B$, $Sm_2(Fe,Co)_{14}B_1$, stoichiometric $TbCu_7$ type phase and $CeCo_4B$ type phase, respectively.

2. EXPERIMENT

The ingots of Sm-Fe-Co-Cu-Nb-B alloys were prepared by arc-melting under Ar atmosphere. The Cu roll surface velocity Vs was set on 18 m/s. For some samples, the melt-spinning with Vs=4~8 m/s was tested. The as-spun ribbons were annealed at 893~953 K in 10~15 min in Ar atmosphere. The magnetic properties of the annealed ribbons were measured on the pieces 4 mm wide and 6 mm long with a vibrating magnetometer (VSM) applying field up to 1.6 MA/m parallel to the length direction of the ribbons. However, some samples were magnetized at 5.6 MA/m before measuring. Powder X-ray diffraction (XRD) measurements with Cu-Kα radiation were carried out for determining the crystal structures of the samples.

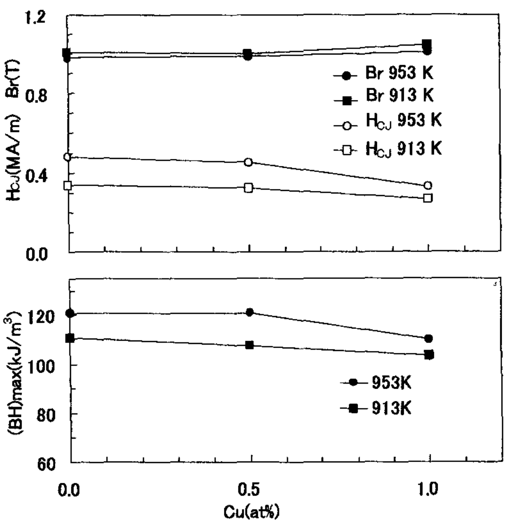

Fig.1. H_{CJ}, Br and $(BH)_{max}$ dependences on Cu content of $Sm_{6.5}Fe_{bal.}Co_{20}Cu_xNb_3B_8$ (x=0, 0.5, 1.0) ribbons.

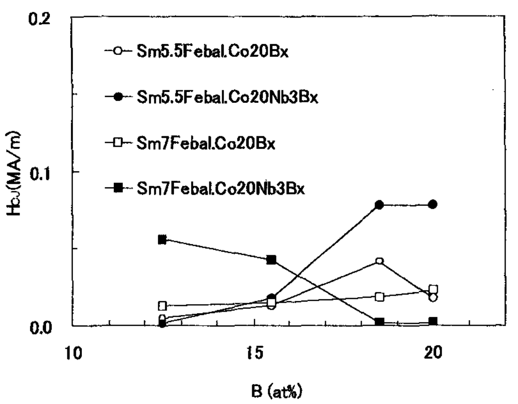

Fig.2. H_{CJ} for Cu-free $Sm_xFe_{bal.}Co_{20}Nb_yB_z$ (x=5.5, 7.0, y=0, 3, z=12.5~20.0) ribbons annealed at the same conditions for Cu-added ribbons.

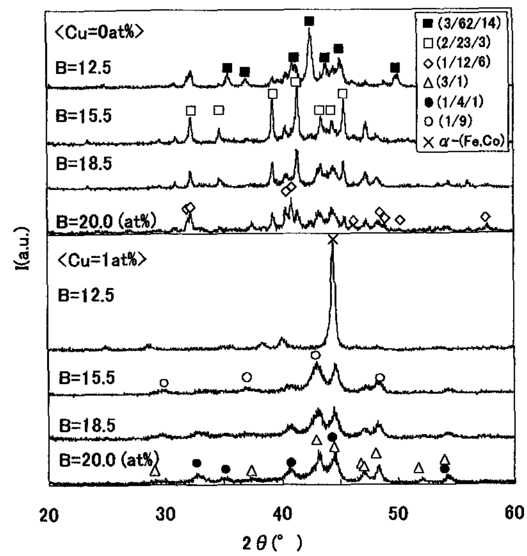

Fig.3. XRD patterns for $Sm_{5.5}Fe_{bal.}Co_{20}Cu_xB_y$ (x=0, 1, y=12.5~20.0) ribbons annealed at 893K for15min.

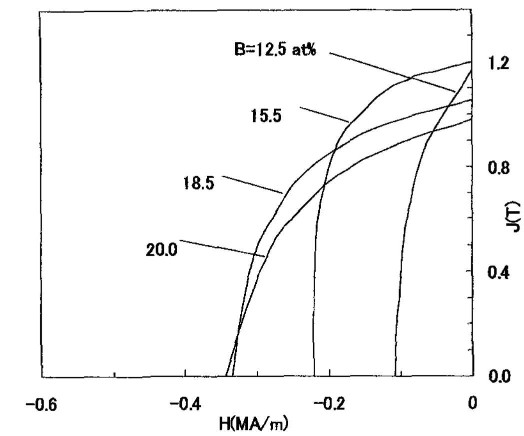

Fig.4. Demagnetization curves for $Sm_{5.5}Fe_{bal.}Co_{20}Cu_1B_x$ (x=12.5~20.0) ribbons annealed at 893K for 15min.

3. RESULTS AND DISCUSSION

3.1 B=8at% case

Fig.1 shows H_{CJ}, Br and $(BH)_{max}$ dependences on Cu content of $Sm_{6.5}Fe_{bal.}Co_{20}Cu_xNb_3B_8$ (x=0, 0.5, 1.0) ribbons annealed at 913, 953 K for 10 min. It is shown that increasing Cu content Br does not change and H_{CJ} decreases slightly in both annealing conditions. These features are similar to the results of α-Fe/$Nd_2Fe_{14}B_1$ nanocomposites. In recent study[6] on the crystallization of nanocomposite $Nd_8Fe_{bal.}Co_8Nb_xCu_yB_6$ (x=0~2.5, y=0, 0.5) magnets, it is found that no evidence for Cu clustering has been found. From the measuring magnetic properties of the ribbons, Cu has no effective role for increasing coercivities.

3.2 B=12.5~20.0 at% case

Fig.2 shows H_{CJ} for Cu-free $Sm_xFe_{bal.}Co_{20}Nb_yB_z$ (x=5.5, 7.0, y=0, 3.0, z=12.5~20.0) ribbons. Annealing conditions are the same as those for the following Cu added ribbons. The obtained H_{CJ} are less than 0.1MA/m.

Fig.3 shows XRD patterns for $Sm_{5.5}Fe_{bal.}Co_{20}Cu_xB_y$ (x=0, 1, y=12.5~20.0) ribbons annealed at 893 K for 15 min. In Cu-free ribbons, cubic 3/62/14, 2/23/3 phases and hexagonal 1/12/6 phase appeared. These phases are known as metastable phases in the crystallization processes in Nd-Fe-B melt spun ribbons. On the contrary to the Cu-free ribbons, completely different structures appeared in Cu=1 at% ribbons. In B=15.5~20.0 at% cases, hard magnetic 1/9 phase, 1/4/1 phase and soft magnetic 3/1 phase appeared. In B=20.0 at% ribbons, no peaks corresponding to 1/9 phase was observed. It is remarkable that no 2/14/1 phase appeared in all these XRD patterns.

Fig.4 shows demagnetization curves for $Sm_{5.5}Fe_{bal.}Co_{20}Cu_1B_x$ (x=12.5~20.0) ribbons annealed at 893K for 15 min. All ribbons show hard magnetic properties, especially 15.5 at% ribbon has the values of Br=1.20 T, H_{CJ}=0.24 MA/m and B=18.5 at% ribbon

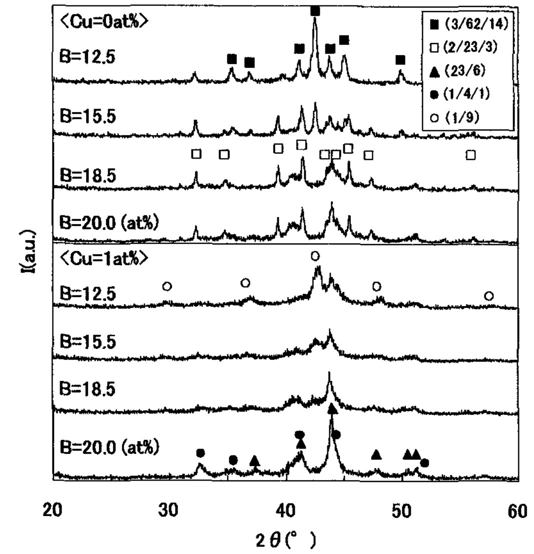

Fig.5. XRD patterns for $Sm_{5.5}Fe_{bal.}Co_{20}Cu_xNb_3B_y$ (x=0, 1, y=12.5~20.0) ribbons annealed at 933K for 15min.

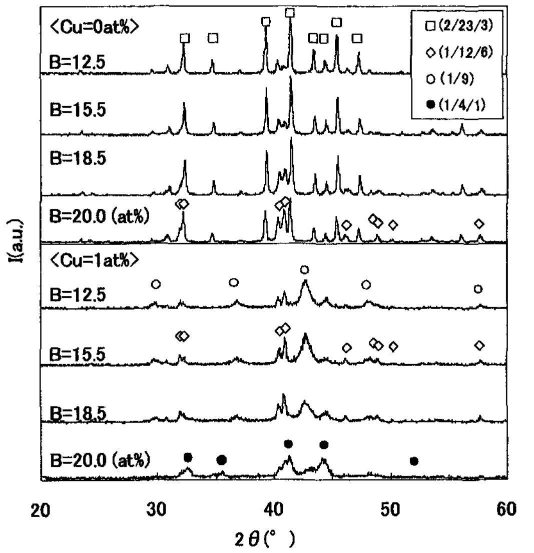

Fig.7. XRD patterns for $Sm_7Fe_{bal.}Co_{20}Cu_xB_y$ (x=0, 1, y=12.5~20.0) ribbons annealed at 913K for 10min.

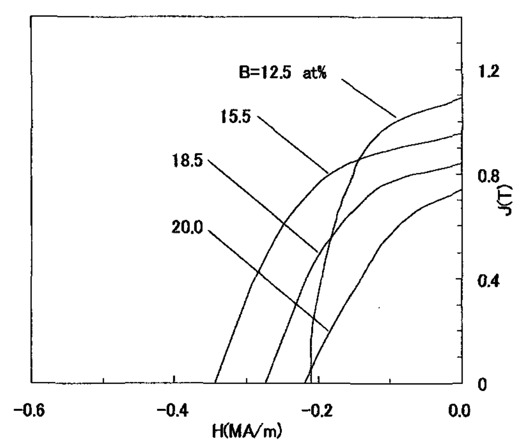

Fig.6. Demagnetization curves for $Sm_{5.5}Fe_{bal}Co_{20}Cu_1Nb_3B_x$ (x=12.520.0) ribbons annealed at 933K for15min.

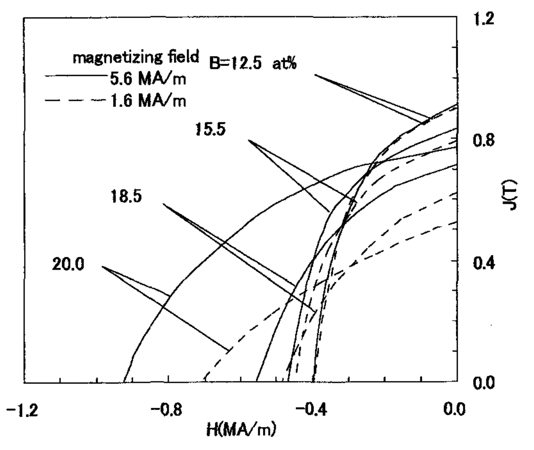

Fig.8. Demagnetization curves for $Sm_7Fe_{bal.}Co_{20}Cu_1B_x$ (x=12.5~20.0) annealed at 913K (x=12.5, 15.5) and 933K (x=18.5, 20.0) for 15min.

shows Br=1.05T, H_{cJ}=0.34 MA/m. These values are similar to those of $Fe_3B/Nd_2Fe_{14}B_1$ spring magnets.

Next, we studied the Cu effect for Nb-doped (3at%) ribbons. Fig5. shows the XRD patterns for $Sm_{5.5}Fe_{bal.}Co_{20}Cu_xNb_3B_y$ (x=0, 1, y=12.5~20.0) ribbons annealed at 933K for 15 min. In Cu free ribbons, cubic 3/62/14 and 2/23/3 phases appeared without hexagonal 1/12/6. Increasing B content from 12.5at% to 20.0 at%, the intensity of 3/62/14 phase decreased and that of 2/23/3 phase increased. On the other hand, only 1at% Cu addition drastically changed crystal structure. Instead of 3/62/14, 2/23/3 phases, hard magnetic 1/9 and 1/4/1 phases appeared with soft magnetic 23/6 phase instead of soft magnetic 3/1 phase observed in Nb-free ribbon.

Fig.6 shows demagnetization curves for $Sm_{5.5}Fe_{bal.}Co_{20}Cu_xNb_3B_y$ (x=0, 1, y=12.5~20.0) ribbons annealed at 933K for 15 min. Maximum coercivity is H_{cJ}=0.35 MA/m for B=15.5 at% sample, but Br was less than 1T. Comparing the Nb-free cases, there has no effective role for Nb addition.

For increasing coercivity, Sm-rich (7at%) composition was examined. Fig. 7 shows XRD patterns for $Sm_7Fe_{bal.}Co_{20}Cu_xB_y$ (x=0, 1, y=12.5~20.0) ribbons annealed at 913 K for 10min. In Cu-free ribbons, 2/23/3 phase and 1/12/6 phase appeared as in the case of Sm=5.5at%. However, 3/62/14 phase was not seen. In Cu=1 at% ribbons, 1/9, 1/4/1 hard magnetic phases appeared with hexagonal 1/12/6 phase.

Fig. 8 shows demagnetization curves for $Sm_7Fe_{bal.}Co_{20}Cu_1B_x$ (x=12.5~20.0) ribbons annealed at 913 K (x=12.5, 15.5) and 933 K (x=18.5, 20.0) for 15 min. Though the coercivities of x=12.5~18.5 ribbons still remain in 0.4~0.55 MA/m, higher values more than 0.9MA/m was obtained after magnetizing B=20.0 at% sample with 5.6MA/m field. However, as can be seen in Fig. 8, B=18.5, 20.0at% ribbons show low magnetizability. In the case of 1.6MA/m field, Br and H_{cJ} for B=20.0 at% sample are 0.52 T and 0.7 MA/m,

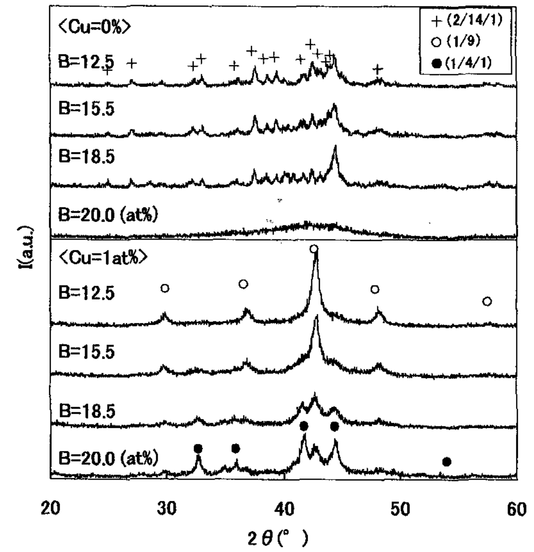

Fig.9. XRD patterns for $Sm_7Fe_{bal.}Co_{20}Cu_xNb_3B_y$ (x=0, 1, y=12.5~20.0) ribbons annealed at 933K for 15min.

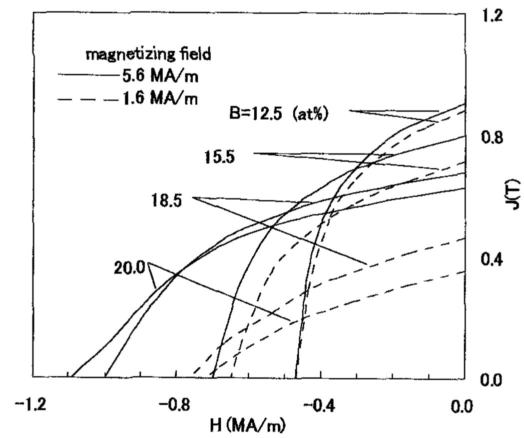

Fig.10. Demagnetization curves for $Sm_7Fe_{bal.}Co_{20}Cu_1Nb_3B_x$ (x=12.5~20.0) ribbons annealed at 933K for 15min.

respectively. This implies that hard magnetic 1/4/1 phase has too large anisotropy field H_A to magnetize isotropic crystalline ribbons easily.

Fig.9 shows XRD patterns for Sm-rich Nb-doped $Sm_7Fe_{bal.}Co_{20}Cu_xNb_3B_y$ (x=0, 1, y=12.5~20.0) ribbons annealed at 933K for 15 min. In Cu free ribbons, tetragonal 2/14/1 phase appeared for B=12.5~18.5 at% ribbons and amorphous state is observed in B=20.0 at% sample. On the other hand, Cu-added samples show 1/9 phase and 1/4/1 instead of 2/14/1 phase. Comparing Fig.9 with Fig.7, (Cu, Nb)-doped ribbons show no hexagonal 1/12/6 phase.

Fig.10 shows demagnetization curves for $Sm_7Fe_{bal.}Co_{20}Cu_xNb_3B_y$ (x=0, 1, y=12.5~20.0) ribbons annealed at 933 K for 15 min. Increasing B content of the samples, H_{cJ} reaches maximum value of 1.3 MA/m in B=20at% sample. Comparing with the results of Nb-free case, H_{cJ} is larger than that of corresponding value in every B content. This is attributed to the

Table I. Roll surface velocitiesVs , ribbon thickness and magnetic properties (annealing: 913K for 10min.).

Vs (m/s)	Thickness (μm)	H_{cJ} (MA/m)	Br (T)	$(BH)_{max}$ (kJ/m^3)
8	75~90	0.32	1.08	124
6	95~115	0.34	1.07	122
4	120~160	0.33	1.08	124

disappearance of 1/12/6 phase in Nb-doped samples.

3.3 Roll surface velocity

These alloys have a large B content, so it is expected that lower roll surface velocity less than 18m/s to be applicable. Table I shows roll surface velocities Vs, ribbon thickness and magnetic properties for $Sm_{5.5}Fe_{bal.}Co_{20}Cu_1B_{18.5}$ ribbons spun at Vs=4~8m/s. It has been confirmed that every sample is amorphous in as-spun state. As can be seen in Table I, obtained magnetic properties are the same after annealing at 913K for 10min. The ribbon thickness larger than 100μm is obtained at the roll surface velocity less than 6m/s.

4. CONCLUSION

The magnetic properties and crystal structures of Sm-Fe-Co-Cu-Nb-B melt-spun ribbons annealed at suitable conditions have been investigated. It is found that Cu addition has different effects on coercivities for the alloys of B=8 at% and B=12.5~20.0 at%. Cu addition has no beneficial effect to increase the coercivities for $Sm_{6.5}Fe_{bal.}Co_{20}Cu_1Nb_3B_8$ ribbons. On the other hand, to the alloys containing more B-rich compositions; $Sm_xFe_{bal.}Co_{20}Cu_1Nb_yB_z$ (x=5.5, 7, y=0, 3, z=12.5~20.0), Cu addition has an essential role not only for increasing coercivities but also for changing crystal structures of the ribbons.

REFERENCES

[1] Y. Yoshizawa, S. Oguma and K. Yamauchi, J. Appl. Phys., **64**, 6044-6046 (1988).

[2] Z. Chen, Y. Zhang, Y. Ding, G.C. Hadjipanayis, Q. Chen and B.M. Ma, J. Magn. Magn. Mater., **195**, 420-427 (1999).

[3] M. Hamano, M. Yamasaki, H. Mizuguchi, H. Yamamoto and A. Inoue, Proc. 15th Int. Workshop on Rare-Earth Magnets and Their Applications, Ed. by L. Schultz and K.H. Muller, 199-204 (1998).

[4] D. H. Ping, K. Hono, H. Kanekiyo and S. Hirosawa, Acta mater., **47**, 4641-4651 (1999).

[5] T. Miyoshi, H. Kanekiyo and S. Hirosawa, Proc. 16th Int. Workshop on Rare-Earth Magnets and Their Applications, Ed. by H. Kaneko, M. Homma and M. Okada, 495-504 (2000).

[6] D. H. Ping, Y. Q. Wu, H. Kanekiyo, S. Hirosawa and K. Hono, Proc. 16th Int. Workshop on Rare-Earth Magnets and Their Applications, Ed. by H. Kaneko, M. Homma and M. Okada, 505-512 (2000).

[7] M. Mochizuki, M. Shimizu, M. Murakawa and S. Tanigawa, Proc. 17th Int. Workshop on Rare-Earth Magnets and Their Applications, Ed. by G. C. Hadjipanayis and M.J. Bonder, 401-408 (2002).

(Received October 8, 2003; Accepted January 13, 2004)